Comparison of Global Positioning System and Water Vapor Radiometer Wet Tropospheric Delay Estimates

R. Linfield, Y. Bar-Sever, and P. Kroger
Tracking Systems and Applications Section

S. Keihm
Microwave, Lidar, and Interferometer Technology Section

Comparison of simultaneous Global Positioning System (GPS) and water vapor radiometer (WVR) measurements at Goldstone over 82 days in the period between June 25 and October 6, 1996, shows agreement in zenith wet path-delay estimates to <6 mm rms. The level of agreement is consistent with the expected levels of GPS and WVR errors. This method shows considerable promise for improving the accuracy of the water vapor emission model. Future GPS/WVR measurements at a wet site using one additional instrument (a microwave temperature profiler) are expected to reduce the uncertainty in this emission model to <2 percent.

I. Introduction

The Earth's troposphere causes a refractive delay at microwave frequencies of approximately 7 ns at the zenith, equivalent to an excess path length of 2 m. Any precision phase or delay measurements at microwave frequencies that involve signals propagating between space and the ground must include a means of calibrating the effect of the troposphere.

It is convenient to divide the tropospheric delay into two components: dry and wet. The large majority of the delay (typically $\geq$90 percent) is due to the dry component of the air (mainly nitrogen and oxygen). Because dry air is well mixed, variations in the dry delay mostly are slow and smooth. The refractivity of dry air [1] is almost perfectly proportional to density. Therefore, under the assumption of hydrostatic equilibrium, the dry delay can be derived very simply from the surface pressure, with an uncertainty of $\approx$0.5 mm [2].

The contribution from water vapor is less than $\approx$40 cm for nearly all locations on Earth at any time. For DSN sites, the average zenith wet delay is $\sim$10 cm. However, because the distribution of atmospheric water vapor is highly inhomogeneous, almost all the high-frequency temporal and spatial variability in the total tropospheric path delay at any site is due to variations in wet delay.

There is strong interest in calibration of the wet delay (in the zenith direction, averaged over the sky, or, more generally, along any desired line of sight). The variable wet delay is an important error source for any precise delay or phase measurements made along space–ground paths at microwave frequencies. One

important class of such observations comes from radio science experiments made with DSN antennas and planetary spacecraft. The Cassini spacecraft will have a multiple frequency capability to support radio science experiments, with Ka-band (∼32 GHz) as its highest frequency. This capability will allow the dispersive effects of ionized media (the interplanetary medium and the Earth's ionosphere) to be removed almost perfectly. The nondispersive effects of the Earth's troposphere will, therefore, be a much more dominant error source than for radio science experiments with earlier spacecraft (which were performed at lower frequencies).

A second motivation for calibration of the wet delay arises from its use in weather forecasting and climate modeling. For these purposes, the wet delay often will be converted to precipitable water vapor.

The two principal calibration techniques use (1) water vapor radiometers (WVRs) and (2) Global Positioning System (GPS) receivers. WVRs [e.g., 3] measure the brightness temperature of the sky at two or more frequencies in the vicinity of the 22-GHz water vapor spectral line and use these measurements, and an assumed model for atmospheric vapor absorption, to infer the water vapor-induced delay. GPS receivers [4] observe dual-frequency transitions from multiple GPS satellites (typically 5 to 8 at any one time). Observations from a period of ≥24 hours can be used to solve for multiple parameters, including mean (sky-averaged) total (wet + dry) zenith tropospheric delay as a function of time. The dry zenith delay can be obtained from surface pressure measurements. Subtracting the dry delay from the total tropospheric delay gives the GPS-derived wet delay.

In order to test the accuracy of these two methods for measuring the wet delay, we conducted simultaneous WVR and GPS measurements for 4 months at the DSN station in Goldstone, California.

II. Observations and Data Reduction

From late June until early December, 1996, two water vapor radiometers and two GPS receivers operated continuously at Goldstone (DSS 13). The two WVRs were of different designs: one R-unit and one J-unit [5]. The GPS receivers were Allen Osborne Turbo Rogues (model numbers SNR 8000 and SNR 8100), with choke ring antennas. This article covers the data collected between June 25 and October 5.

One WVR (the J-unit) was located near the 34-m DSS-13 antenna, while the other (R-unit) was located near the control building. Both GPS antennas were located within 50 m of the R-WVR, one on a ground tripod and one on the control building roof. The J-WVR was approximately 300 m from the other instruments. A surface meteorology package (Paroscientific Inc., model 6016B) included a pressure and temperature sensor. The expected zenith wet delay difference at Goldstone for a 300-m horizontal offset is <0.5 mm for short integration times (<10 s) and <0.15 mm for averaging times ≥10 min [6].

A. Water Vapor Radiometers

Both WVRs operated continuously in "tip-curve" mode to provide precise monitoring of instrument gain variations. Measurements of sky brightness temperature were made sequentially at three elevation angles—90, 42, and 30 deg—and four azimuths.

The brightness temperatures in the zenith were used to derive wet zenith delays at 3- to 4-minute intervals. Several statistical retrieval algorithms [e.g., 7] were used. A large database of radiosonde flights was used to generate the correlation between wet delays and various observables for a location (Desert Rock, Nevada) with a climate similar to that of Goldstone. All of our retrieval algorithms for both WVRs used brightness temperatures at 20.7 and 31.4 GHz (brightness temperatures at the 22.2-GHz line center are less useful, because they are very sensitive to the height distribution of the water vapor). In addition, some algorithms used the instantaneous and/or the 24-hour average surface temperature. The motivation for using a time average surface temperature is to give a better approximation to the mean

temperature of the wet troposphere than is provided by the instantaneous surface temperature, which has large diurnal variations. All of these retrieval algorithms gave very nearly the same results, with differences much smaller than the GPS–WVR wet delay differences reported below. Algorithms with the 24-hour average surface temperatures gave the best statistical retrieval performance (as quantified by the residuals to the linear fits used in generating the algorithm, as well as by the variance of the GPS–WVR differences). We also tried a Bayesian retrieval algorithm. Although such algorithms give performance superior to a statistical algorithm when full temperature profiling is available [8], they produced only marginal improvement for our case, where only surface temperatures were available. The results presented in this article used these Bayesian retrievals for the WVR data.

We eliminated all data that showed evidence of clouds in the zenith direction. In principle, a two-frequency WVR can remove the effect of cloud emission and produce an accurate wet path-delay retrieval. In practice, mismatch between the beam patterns at the two frequencies causes significant errors in such retrievals. The criterion for data exclusion was a derived level of integrated cloud liquid $\geq 20\mu$m, using a linear regression formula dependent on the WVR brightness temperatures.

B. GPS Receivers

Data from each receiver were sampled every 5 minutes. These data were used (in 30-hour blocks for each receiver) to solve for a mean receiver location, a clock offset, and a zenith tropospheric delay every 5 minutes. This analysis used satellite orbits and clocks derived from a global GPS ground network's solutions using the point-positioning technique [9]. Most of these global solutions were 30 hours in length, and all of them were centered on UT 12:00. As described later, we also tried longer solutions. In all our solutions, we used all data where the satellite elevation angle was larger than 7 deg. The minimum elevation angle is a trade-off. Lower minimum elevation angles result in a lower signal-to-noise ratio (SNR) and larger multipath problems. However, the correlation between zenith tropospheric delays and other parameters (especially receiver location) is large at high elevation angles. Therefore, use of low elevation angle data helps to break this correlation among parameters. Extensive tests for many ground sites have shown that a GPS elevation angle cutoff of 7 deg gives better internal consistency (e.g., smaller scatter in the solutions for receiver location) than with a 15-deg cutoff.

Surface pressure measurements were used to derive the dry tropospheric delay. This was subtracted from the total GPS tropospheric delay to get the wet delay, using the standard conversion [2]. The height of the pressure sensor differed by <2 m from the height of the GPS antennas. The pressures were corrected to the height of the antennas by assuming a pressure scale height of 8 km (e.g., when the pressure sensor was 77 cm below one antenna, the pressure values were multiplied by $e^{-0.77/8000}$, corresponding to a zenith delay correction of $\approx$0.2 mm). Pressure readings were smoothed with a 30-minute time constant and interpolated to the epochs of the GPS troposphere delay estimates.

III. GPS–WVR Comparisons

Data from the R-series WVR were used for the comparisons because of calibration problems with the J-series WVR. (There was contamination due to thermal emission from a Joshua tree at the lowest elevation angle used in the tip curves.) Of the two GPS receivers, the one with the antenna mounted on the ground tripod yielded smaller postfit residuals from the precise point-position solution described above. We therefore used data from this receiver in our comparisons.

We did not have all three types of data (GPS, WVR, and surface pressure/temperature) available at all times. During the period between June 25 and October 5, there were four segments, ranging in length from 11 to 41 days, when we had all three data types. The sum of the length of the data segments was 86 days. The span of dates for each segment is shown in Table 1.

The WVR wet delays were interpolated to the epoch of the GPS wet delay for comparison. The four segments of data are shown in Figs. 1 through 4. For these data, 30-hour global GPS solutions were used.

Table 1. Epochs of the data segments.

Segment	Range of dates	Length, days
1	June 25–August 6	41.6
2	August 14–August 26	11.9
3	August 27–September 10	13.3
4	September 17–October 6	19.0

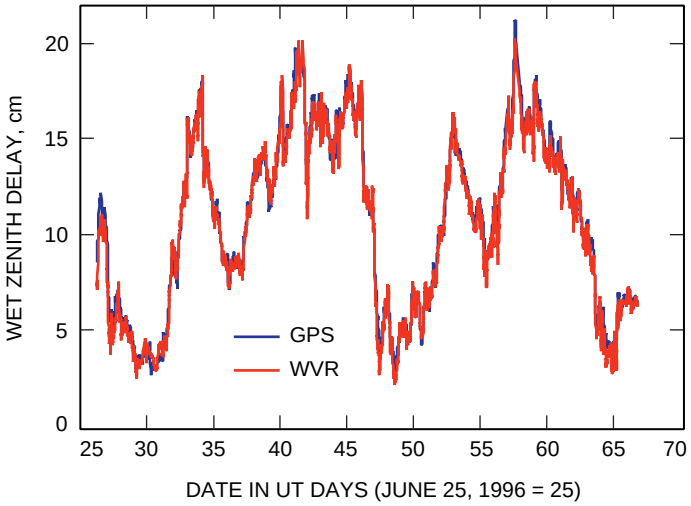

Fig. 1. Time series of GPS and WVR zenith wet path delays for data segment 1.

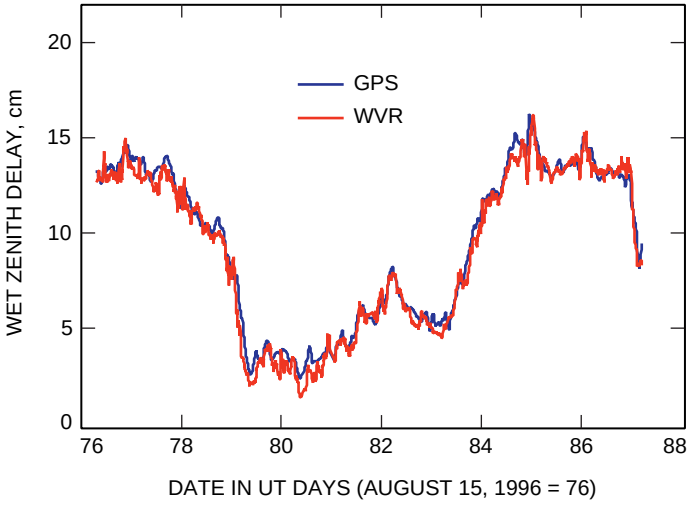

Fig. 2. Time series of GPS and WVR zenith wet path delays for data segment 2.

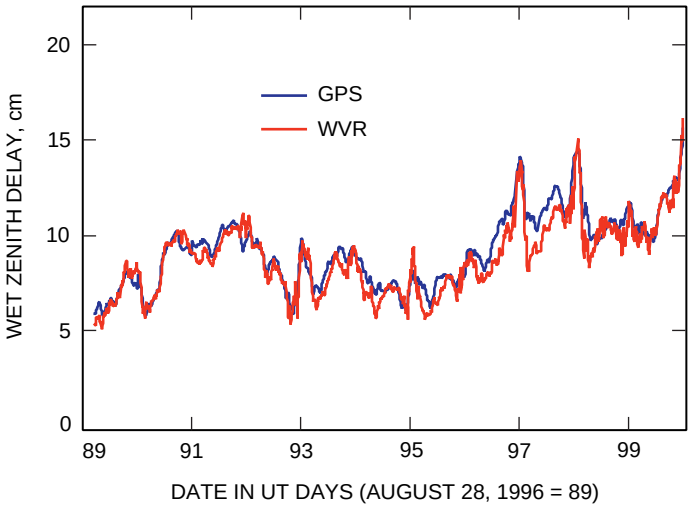

Fig. 3. Time series of GPS and WVR zenith wet path delays for data segment 3.

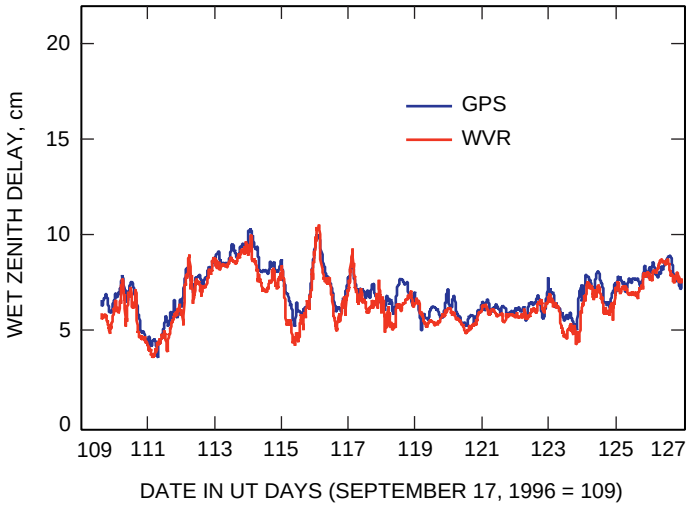

Fig. 4. Time series of GPS and WVR zenith wet path delays for data segment 4.

The mean wet delays and the mean and standard deviation of the GPS–WVR differences are shown in Table 2. Standard deviations are given for both the entire set of data values (one every 5 minutes) and for 24-hour averages (the means of both sets are the same).

IV. Error Sources

The largest contributions to the standard deviations of the GPS–WVR wet path-delay difference are believed to be GPS total troposphere error, WVR retrieval error, and WVR gain calibration error. Each of these three error sources is discussed below.

A. GPS Total Troposphere Delay Errors

The estimated accuracy of GPS troposphere delay estimates is 3 to 4 mm [10]. The largest contribution to the uncertainty in these estimates arises from errors in the GPS orbits. Based on the comparison of

Table 2. Statistics on the GPS–WVR comparison.

Segment	Mean WVR delay, cm	Mean GPS–WVR difference, mm	Standard deviation of 5-min values, mm	Standard deviation of 24-h averages, mm
1	10.5	2.0	5.3	2.9
2	9.2	3.1	5.2	2.2
3	8.8	4.0	6.4	3.3
4	6.6	4.3	4.5	2.1

GPS solutions that are centered on different epochs, but which overlap, the orbit errors are observed to be largest at the edges of solution intervals. In order to look for such an effect, we binned our data by UT. In Figs. 5 and 6, we show the mean and standard deviation within each 10-percent bin of UT (e.g., from UT 00:00 to 02:24 for bin no. 1) for each of the four segments. The standard deviations are largest near UT 0 and 24, consistent with the behavior expected from the contribution of GPS orbit errors, but with a larger magnitude than expected.

B. WVR Retrieval Errors

The conversion from sky brightness temperatures to wet path delays is not unique, because the two quantities depend in different ways upon the temperature and water vapor density along the line of sight. We did not have any measurements of temperature or vapor density profile for this data set, except for surface temperatures. For the mean wet delays of ≈10 cm in our data set, the estimated retrieval errors were 2 to 3 mm, based on the Desert Rock regression fits. In Fig. 5, it can be seen that the mean GPS–WVR difference varies systematically throughout the UT day, with a peak–peak variation of ∼3 mm. We believe that this variation represents one component of the retrieval error. It results from a systematic deviation between the true temperature profile (which varies much more strongly within a day than between days in Goldstone in summer) and the temperature profile used in the Bayesian retrieval algorithm.

C. WVR Gain Calibration Errors

Any errors in calibration of the WVR instrumental gains will translate into brightness temperature errors, and then into wet path delay errors. Based on comparisons between co-located WVRs of different designs, the brightness temperature errors are believed to be 0.2 to 0.3 K, corresponding to <2-mm wet path-delay errors.

As a test of the gain calibration error, we examined simultaneous data from the two WVRs (the J-unit and the R-unit) during 12 days in August, when both instruments were operating simultaneously. The data from the J-unit during this period were carefully edited to correct for the thermal contamination from the Joshua tree mentioned above. The mean GPS–WVR wet delay difference was 3.0 mm with the R-unit and 3.6 or 3.9 mm (depending upon the gain calibration method) with the J-unit. The standard deviation of the difference was the same, 5.4 mm, for all three cases. This suggests that WVR gain calibration errors do not contribute significantly to the overall scatter in GPS–WVR values.

D. Total Error

If we add the errors from these three sources in quadrature, we get 4 to 5 mm, in fairly close agreement with the observed standard deviations. Only the standard deviation from segment 3 is significantly different from our estimated errors; there may have been some unknown systematic error during this period, or some known error may have been larger than expected.

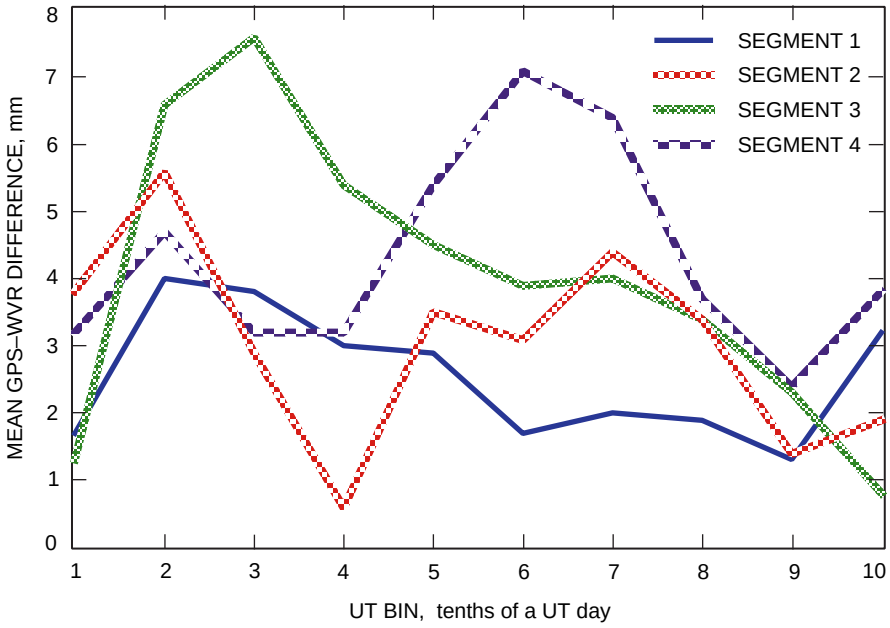

Fig. 5. Mean GPS–WVR differences, binned by tenths of the UT day, for each of data segments 1 through 4.

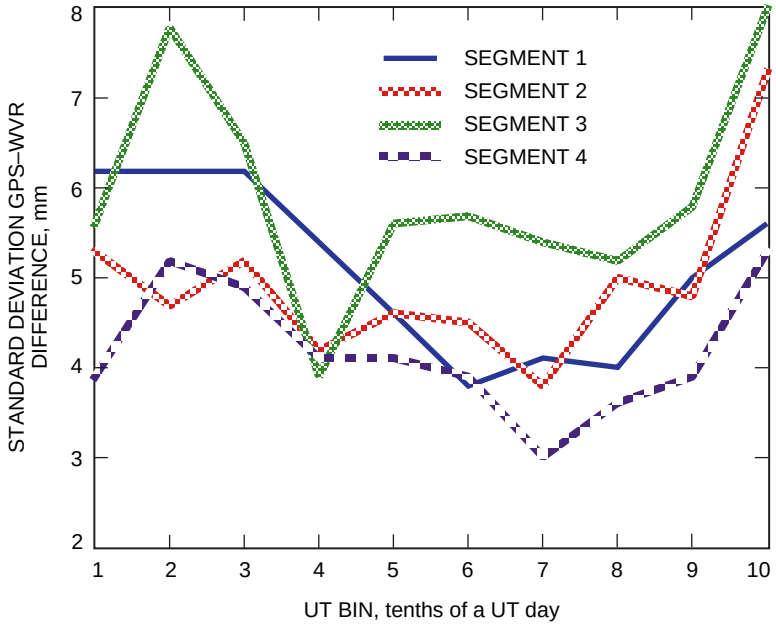

Fig. 6. Standard deviation of GPS–WVR differences, binned by tenths of the UT day, for each of data segments 1 through 4.

V. Improvements to the Water Vapor Emission Model

A major motivation for these measurements was to improve our knowledge of the water vapor emission model, thus allowing improved WVR wet delay calibrations. Any conversion from WVR measurements of brightness temperatures to quantities involving water vapor (e.g., the water vapor column density) depend upon the mass absorption coefficient, κ_ν. The derived wet path delay also is sensitive to the mass

refractivity coefficient, K_3. To elaborate briefly, the spectral emissivity, ϵ_ν, of a parcel of moist air with water vapor density ρ_v and temperature T is

$$\epsilon_\nu = T\rho_v\kappa_\nu$$

The refractivity, N, of this parcel, due to the water vapor, is

$$N \approx \frac{K_3\rho_v}{T}$$

The conversion from measured WVR brightness temperature to estimated wet path delay is proportional to the ratio of coefficients,

$$\frac{K_3}{\kappa_\nu}$$

This coefficient currently is known to an accuracy no better than ≈5 percent, with almost all the uncertainty due to κ_ν. Laboratory measurements of κ_ν are difficult because of the weakness of the 22-GHz spectral line. Comparisons between WVR measurements and radiosonde profiles of temperature and water vapor are limited largely by the accuracy of the vapor sensors. Simultaneous GPS and WVR measurements have the advantages that (1) both are potentially high-accuracy techniques and (2) GPS wet delay estimates do not depend on either κ_ν or K_3.

From Table 2, the ratios of the mean GPS–WVR differences to the mean wet delay are 2.5, 3.3, 4.5, and 6.5 percent for the four segments. We do not understand the spread in these values in a quantitative way, and we do not know if the apparent secular increase is real. Nonetheless, the data suggest that our current value [11] of κ_ν (more specifically, κ_ν/K_3) is too large by 3 to 4 percent.

VI. Future Plans

Our two largest error sources are the errors in the total GPS troposphere delay estimates and the WVR retrieval errors. No simple known change can reduce the first one, but we are investigating some possibilities. However, the second error source can be reduced significantly if we add the capability of temperature profiling during our observations. A microwave temperature profiler [12] can measure the temperature of the wet troposphere to an accuracy of 1 to 2 K. We plan to use one during future measurements.

A warm wet site, such as south Florida or Hawaii, often has wet delays of ≈35 cm. GPS/WVR measurements at such a site (with a microwave temperature profiler) should allow measurements of K_3/κ_ν to an accuracy of 2 percent or better.

Acknowledgments

B. Haines and G. Resch made useful suggestions based on reading a draft version of this article.

References

[1] G. D. Thayer, "An Improved Equation for the Radio Refractive Index of Air," *Radio Science*, vol. 9, pp. 803–807, 1974.

[2] J. L. Davis, T. A. Herring, I. I. Shapiro, A. E. E. Rogers, and G. Elgered, "Geodesy by Radio Interferometry: Effects of Atmospheric Modeling Errors on Estimates of Baseline Length," *Radio Science*, vol. 20, no. 6, pp. 1593–1607, 1985.

[3] G. Elgered, "Tropospheric Radio Path Delay From Ground-Based Microwave Radiometry," Chapter 5, *Atmospheric Remote Sensing by Microwave Radiometry*, edited by M. Janssen, New York: Wiley & Sons, 1993.

[4] A. Leick, *GPS Satellite Surveying*, New York: John Wiley & Sons, 1994.

[5] M. A. Janssen, "A New Instrument for the Determination of Radio Path Delay Due to Atmospheric Water Vapor," *IEEE Trans. Geosci. Remote Sens.*, vol. 23, no. 4, pp. 485–490, 1985.

[6] R. P. Linfield and J. Z. Wilcox, "Radio Metric Errors Due to Mismatch and Offset Between a DSN Antenna Beam and the Beam of a Troposphere Calibration Instrument," *The Telecommunications and Data Acquisition Progress Report 42-114, April–June, 1993*, Jet Propulsion Laboratory, Pasadena, California, pp. 1–13, August 15, 1993.

[7] B. L. Gary, S. J. Keihm, and M. A. Janssen, "Optimum Strategies and Performance for the Remote Sensing of Path-Delay Using Ground-Based Microwave Radiometry," *IEEE Trans. Geosci. Romote Sens.*, vol. 23, pp. 479–484, 1985.

[8] S. J. Keihm and K. A. Marsh, "Advanced Algorithm and System Development for Cassini Radio Science Tropospheric Calibration," *The Telecommunications and Data Acquisition Progress Report 42-127, July–September, 1996*, Jet Propulsion Laboratory, Pasadena, California, pp. 1–20, November 15, 1996. http://tda.jpl.nasa.gov/tda/progress_report/42-127/127A.pdf

[9] J. F. Zumberge, M. B. Heflin, D. C. Jefferson, M. M. Watkins, and F. H. Webb, "Precise Point Positioning for Efficient and Robust Analysis of GPS Data From Large Networks," *J. Geophys. Res.*, vol. 102, no. B3, pp. 5005–5017, 1997.

[10] S. M. Lichten, "Precise Estimation of Tropospheric Path Delays With GPS Techniques," *The Telecommunications and Data Acquisition Progress Report 42-100, October–December 1989*, Jet Propulsion Laboratory, Pasadena, California, pp. 1–12, February 15, 1990.

[11] S. J. Keihm, "Atmospheric Absorption From 20–32 GHz: Radiometric Constraints," *Proceedings of a Specialist Meeting on Microwave Radiometry and Remote Sensing Applications*, edited by E. R. Westwater, U.S. Department of Commerce, National Technical Information Service, Springfield, Virginia, pp. 211–218, 1992.

[12] R. F. Denning, S. L. Guidero, G. S. Parks, and B. L. Gary, "Instrument Description of the Airborne Microwave Temperature Profiler," *J. Geophys. Res.*, vol. 94, no. D14, pp. 16,757–16,765, 1989.